



Article

Tracing Local Production and Agricultural Trade: A Multi-Analytical Study of Roman Amphorae at Conímbriga (Central Portugal)

Ida Buraca ^{1,2}, César Oliveira ^{3,4}, Carlo Bottaini ^{3,4,5}, Vírgilio Hipólito Correia ^{2,6}, Nicola Schiavon ^{3,4}, Iosé Mirão ^{3,4}, and Massimo Beltrame ^{3,4,*}

- Faculty of Arts and Humanities, University of Porto, Via Panorâmica, s/n, 4150-564 Porto, Portugal; up202111470@up.pt
- ² Center for Classical and Humanistic Studies, CECH, Faculty of Arts and Humanities, University of Coimbra, Largo da Porta Férrea, 3004-530 Coimbra, Portugal; virgiliocorreia@mmconimbriga.dgpc.pt
- Laboratório HERCULES, Universidade de Évora, Largo Marquês de Marialva 8, 7000-809 Évora, Portugal; cesar.oliveira@uevora.pt (C.O.); carlo@uevora.pt (C.B.); schiavon@uevora.pt (N.S.); jmirao@uevora.pt (J.M.)
- Laboratório Associado In2Past, Universidade de Évora, Largo Marquês de Marialva 8, 7000-809 Évora, Portugal
- ⁵ CEAACP—Center for Studies in Archeology, Arts and Heritage, Universidade de Coimbra, Colégio de São Jerónimo, Largo de Dinis, 3000-395 Coimbra, Portugal
- ⁶ Conimbriga National Museum, Rua Professor Vergílio Correia, 3150-220 Condeixa-a-Velha, Portugal
- * Correspondence: massimo@uevora.pt

Abstract

Amphorae are a significant type of Roman pottery, serving as both transport containers and indicators of economic and technological practices across the Empire. Despite their importance in interpreting local economic dynamics in Roman Lusitania, the production origins, technological characteristics and functional roles of amphorae from Conímbriga in Portugal remain poorly understood. Previous research has focused primarily on typological comparisons with imported forms, providing limited insight into whether these vessels were produced locally or how they were incorporated into regional trade and agricultural systems. This study takes a multi-analytical approach to examine a group of ten amphorae dating from the 1st to the 5th century AD. While these vessels formally resemble wellknown types from Gaul and Hispania, they appear to have been manufactured locally using fabrics consistent with those found in regional common wares. To examine the raw materials, production techniques and possible contents, the analysis integrates a typological assessment with a range of archaeometric methods, including optical microscopy (OM), X-ray diffraction (XRD), X-ray fluorescence (XRF) and scanning electron microscopy with energy-dispersive spectroscopy (SEM-EDS). Recent gas chromatography-mass spectrometry (GC-MS) results contextualise these data further, enabling an exploration of how specific technological choices may have influenced or reflected the intended function of the amphorae. The findings shed new light on local ceramic production and contributed to broader debates concerning Roman provincial economies and material culture.

Keywords: amphorae; Roman economy; ceramics production; chemical analysis



Academic Editor: Silvano Mignardi

Received: 12 August 2025 Revised: 20 September 2025 Accepted: 22 September 2025 Published: 28 September 2025

Citation: Buraca, I.; Oliveira, C.; Bottaini, C.; Correia, V.H.; Schiavon, N.; Mirão, J.; Beltrame, M. Tracing Local Production and Agricultural Trade: A Multi-Analytical Study of Roman Amphorae at Conímbriga (Central Portugal). *Heritage* 2025, 8, 405. https://doi.org/10.3390/ heritage8100405

Copyright: © 2025 by the authors. Licensee MDPI, Basel, Switzerland. This article is an open access article distributed under the terms and conditions of the Creative Commons Attribution (CC BY) license (https://creativecommons.org/licenses/by/4.0/).

1. Introduction

The Roman city of Conímbriga is located in central Portugal, within the municipality of Condeixa-a-Nova (district of Coimbra). Since 1930, it has been the focus of systematic

Heritage 2025, 8, 405 2 of 14

archaeological excavations, which have brought to light one of the most significant urban centres of Roman Lusitania (Figure 1).

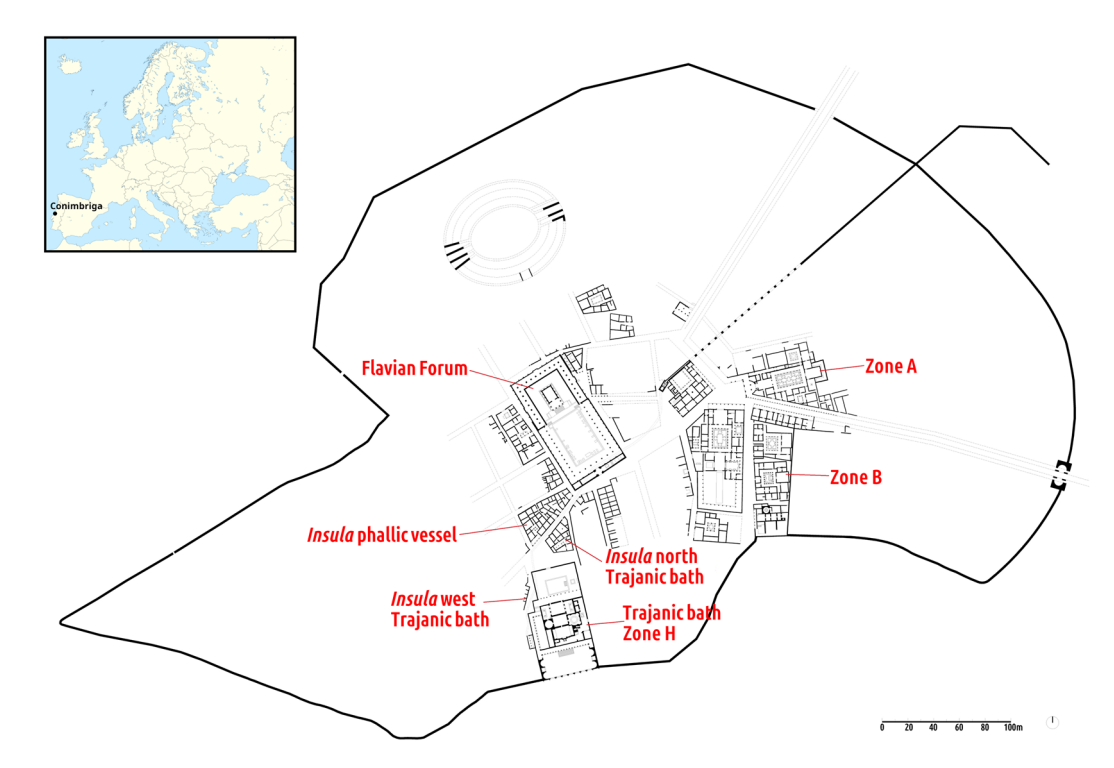


Figure 1. Plan of the Roman city of Conímbriga in the Flavian period (drawing: Virgílio H. Correia, Pedro Alarcão. Execution: Cruz & Alarcão Arquitectos Lda, 2006. © IPM/Museu Monográfico de Conímbriga).

The area, later occupied by the city of Conímbriga, was already settled in Late Prehistory, with archaeological evidence pointing to a Late Bronze Age occupation and the presence of an Iron Age *oppidum*. Following the military campaign of *Decimus Junius Brutus*, the region gradually came under Roman influence, and around 27 BC it was formally integrated into the newly established province of Lusitania [1].

Under Roman rule, a new city was founded and underwent substantial expansion over the following centuries. From the end of the 1st century BC, a comprehensive Augustan urban development programme was launched, including the construction of major infrastructures such as a defensive wall, an aqueduct, a road network, a Forum, and public baths. Archaeological evidence suggests that this phase of construction began around 10 BC [2].

A significant urban transformation occurred between the Flavian period and the 2nd century AD, during the reign of Emperor Vespasian. This development was likely linked to the extension of Latium Minus to the whole of Hispania and to the granting of the honorary title Flavia to the city of Conímbriga [3]. In this period, the Forum was extensively remodelled and expanded, becoming a sanctuary dedicated to the imperial cult in the final quarter of the 1st century AD. The so-called Trajanic Baths were probably constructed shortly after the Forum's renovation, in the early 2nd century AD [4].

The Late Imperial period appears to have begun with the construction of a new defensive wall that reduced the city's perimeter—an intervention generally interpreted as a response to increasing external threats. This fortification has been dated to the late 3rd or early 4th century AD [5]. Despite suffering Suevic attacks in 465 and 468 AD—which resulted in the destruction of several buildings and the capture of the wife and children of Cantaber, a prominent local figure—the city continued to be inhabited [6]. Stratigraphic evidence from substantial rubbish deposits suggests a concentration of population during

Heritage 2025, 8, 405 3 of 14

this period. Between 561 and 580 AD, Conímbriga became the seat of a district under Bishop Lucentius. Radiocarbon dating of the latest occupational phases confirms continued settlement at the site until at least the 12th century AD [7].

The reconstruction of Conímbriga's long-term occupation has been made possible thanks to systematic archaeological investigations. A milestone in this process was the publication, in 1976, of the results of the Portuguese–French excavations conducted between 1964 and 1973, collected in *Fouilles de Conimbriga* [8]. This work marked the beginning of an intensive research program focused on the site's ceramic assemblages. By combining typological and archaeometric approaches, it enabled the identification of locally produced orange common wares. However, due to the highly fragmented nature of the material, amphorae remained among the least thoroughly studied ceramic classes, leaving this area of research relatively underdeveloped.

Nonetheless, some ceramic finds provide indirect evidence for the exportation of agricultural goods produced on a local or regional scale. The presence of dolia—large ceramic containers typically used for the production and storage of wine and olive oil—points to agricultural activity in the area [1,9,10]. Moreover, the limited number of imported oil amphora recovered at Conímbriga suggests a pattern of local production and a likely distribution network operating on a regional scale. The low importation of wine amphorae dated to the late 1st and early 2nd centuries AD further supports the existence of regional commercial circuits for agricultural surplus.

Given that the economy of a Roman city was fundamentally rooted in agriculture, it is plausible that products such as wine, olive oil, and cereals were intended not only for local consumption but also for redistribution. Investigating the provenance of amphorae from Conímbriga therefore offers a valuable opportunity to enhance our understanding of the city's economic role within its territory and the broader dynamics of production and distribution in Roman Lusitania.

As part of a recent chrono-typological reassessment, a group of amphorae exhibiting consistent manufacturing features has been identified, despite their typological variability (10). These include Dressel 2–4, flat-bottomed forms comparable to Gauloise 4 and 5, and Dressel 28, as well as several regionally defined types provisionally designated as Conimbriga 1, Conimbriga 2, and Conimbriga 45/46. Hundreds of amphora fragments were examined macroscopically, with particular attention to ceramic fabrics and temper inclusions. From this assemblage, a representative subset of ten amphorae was selected to reflect a broad spectrum of typological and chronological variation. The primary objective was to establish a robust analytical protocol to determine whether these amphorae were locally produced, and to assess how their technological characteristics and raw materials correspond to regional ceramic traditions.

To address these questions, an integrated, multi-analytical methodology was applied. This approach combined traditional typological analysis with a suite of archaeometric techniques, including optical microscopy (OM), X-ray diffraction (XRD), X-ray fluorescence (XRF), and scanning electron microscopy coupled with energy-dispersive spectroscopy (SEM-EDS). Additionally, these archaeometric data were integrated with the results of recently published gas chromatography–mass spectrometry (GC–MS) analyses carried out on four of the amphora fragments included in the present study. This integration was aimed at exploring how specific technological choices may have influenced, or reflected, the intended function of these vessels within local and regional economic systems.

Heritage 2025, 8, 405 4 of 14

2. Materials and Methods

2.1. Materials

The archaeometric analysis focused on a total of ten amphora fragments representing a typologically diverse group of forms commonly associated with the Roman Imperial period. The sample includes one fragment of Conimbriga 1, two of Dressel 2–4, one of Dressel 28, three of Gauloise 4, one of Conimbriga 2, and two of Conimbriga 45/46 (Figure 2).

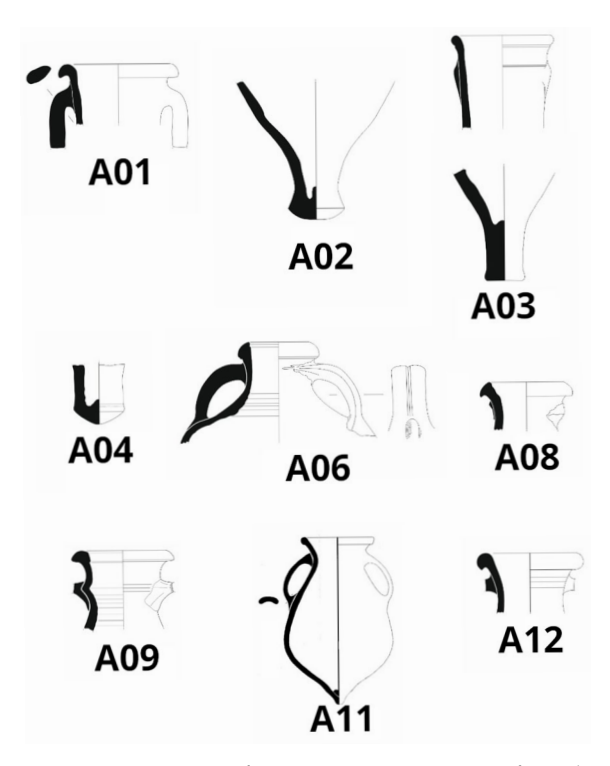


Figure 2. Drawings of a representative group of amphorae analysed in this paper.

Chronologically [1,8–10], the assemblage spans the 1st to 5th centuries AD (Table 1). The selection was based on typological criteria, with the aim of assembling a representative sample relevant to local production and regional distribution dynamics during the Roman occupation.

Roman occupation.	
Table 1. Summary of the analyzed amphora fragments.	

Lab ID	Archaeological ID	Type	Chronology
A01	2004_IWT_2	Conimbriga 1	27 BC to 68 AD
A02	2004_IWT_4	Dressel 2-4	1st century AD (from 69 to 96 AD)
A03	66_H_VI_44_6	Dressel 2-4	1st century AD (from 69 to 96 AD)
A05	67_H_VI_43_9	Dressel 28	Prior to the 3rd century AD
A06	66_U_11	Gauloise 4	Prior to the end of the 3rd century AD
A08	66_F_1/67/12	Gauloise 4	Prior to the end of the 3rd century AD
A09	69_H_VIII_47_5	Conimbriga 2	4th century AD to last quarter of 5th century AD (from 305 to 476 AD)
A10	72_BF6_10	Conimbriga 45-46	Last quarter of the 1st century AD to the 3rd century AD
A11	71_CRY_Norte_Cano	Conimbriga 45-46	Last quarter of the 1st century AD to the 3rd century AD
A12	72_BF1_7	Gauloise 4	Prior to the end of the 3rd century AD

A preliminary macroscopic examination was undertaken to identify variations in ceramic fabric, texture, and firing conditions. Based on visual and tactile assessments, the

Heritage 2025, 8, 405 5 of 14

fragments were classified according to their technological attributes and differences in raw material preparation.

Most samples—specifically A01, A02, A03, A05, A06, A08, and A12—exhibit a very hard and compact red-brown paste, consistent with firing in an oxidizing atmosphere. These fabrics are notably homogeneous and contain very few non-plastic inclusions, suggesting the use of well-processed clays and a controlled production environment.

By contrast, samples A11, A09, and A10 display significantly coarser textures. Their matrices contain abundant large inclusions—both opaque and transparent—alongside small reddish particles and a notable presence of shiny, mica-like minerals. These features indicate different choices in clay selection and preparation. Sample A11 (Conímbriga 45/46 type) shares many of these characteristics but is distinguished by an even higher density of coarse inclusions and mica flakes. Such traits may point to a distinct geological source or to a separate production tradition within the broader ceramic landscape.

This macroscopic classification provided the foundation for the subsequent analytical investigations, which aimed to refine the technological characterization of the fabrics and assess their implications for ceramic production strategies and regional supply systems.

2.2. Methods

To refine the preliminary macroscopic observations and gain deeper insight into the technological characteristics of the ceramic assemblage, a set of complementary analytical techniques was employed. These methods enabled the investigation of mineralogical composition, chemical signatures, and microstructural features through OM, XRD, XRF, and SEM-EDS. The integrated application of these techniques provided a robust analytical framework for reconstructing raw material selection and manufacturing processes.

2.2.1. Optical Microscopy

Petrographic analysis was conducted on thin sections using a Leica DM-2500P polarised light microscope equipped with an image acquisition system. Descriptions of the clay matrix, non-plastic inclusions (i.e., temper), porosity, and temper abundance determination follow the description scheme proposed by Quinn [11]. Grain size classification was based on the Wentworth scale [12].

2.2.2. X-Ray Diffraction

XRD analyses were carried out on powdered samples using a BrukerTM AXS D8 Discovery diffractometer (Da Vinci design), equipped with a Cu K α radiation source (λ = 1.5406 Å), operating at 40 kV and 40 mA, and fitted with a LynxEye 1D detector. Scans were recorded over a 3–75° 20 range, with a step size of 0.05° 20 and an acquisition time of 1 s per step. Mineral identification was performed using Diffract EVA 5.0 software and the PDF-2 database (ICDD). The resulting mineralogical profiles were interpreted with particular attention to high-temperature phase transformations, in order to reconstruct the thermal history of the ceramic pastes.

2.2.3. X-Ray Fluorescence

Major oxides and trace elements concentrations were determined using a Bruker $^{\text{TM}}$ S2 PUMA energy-dispersive X-ray fluorescence (ED-XRF) spectrometer fitted with a silver tube. The instrument was calibrated using 36 certified reference materials. Samples were analysed as fused glass beads, prepared using a 1:10 sample-to-flux ratio. Quantitative data were processed using Spectra Elements 2.0 software. Loss on ignition (LOI) was measured by calcining approximately 1 g of powdered sample at high temperature.

2.2.4. Scanning Electron Microscopy with Energy-Dispersive Spectroscopy

Microstructural and chemical characterization of the ceramic matrix was performed using a HitachiTM S-3700N variable pressure SEM, equipped with a BrukerTM XFlash 5010 silicon drift EDS detector (resolution: 129 eV at FWHM/Mn K α). Analyses were conducted at an accelerating voltage of 20 kV, beam current of 120 μ A, and chamber pressure of 40 Pa. Elemental data were converted to oxides by stoichiometric calculation and normalised to 100%, based on three replicate measurements per sample. Data acquisition and interpretation were carried out using Esprit 1.9 software (Bruker).

3. Results and Discussion

3.1. Technological Analysis and Raw Material Characterization

Petrographic observations conducted under optical microscopy revealed marked compositional and textural variability among the samples, allowing their classification into two main fabric groups (Figure 3). These differences provide insight into raw material procurement strategies, clay preparation techniques, and firing conditions. Full petrographic data are presented in Tables 2–4.

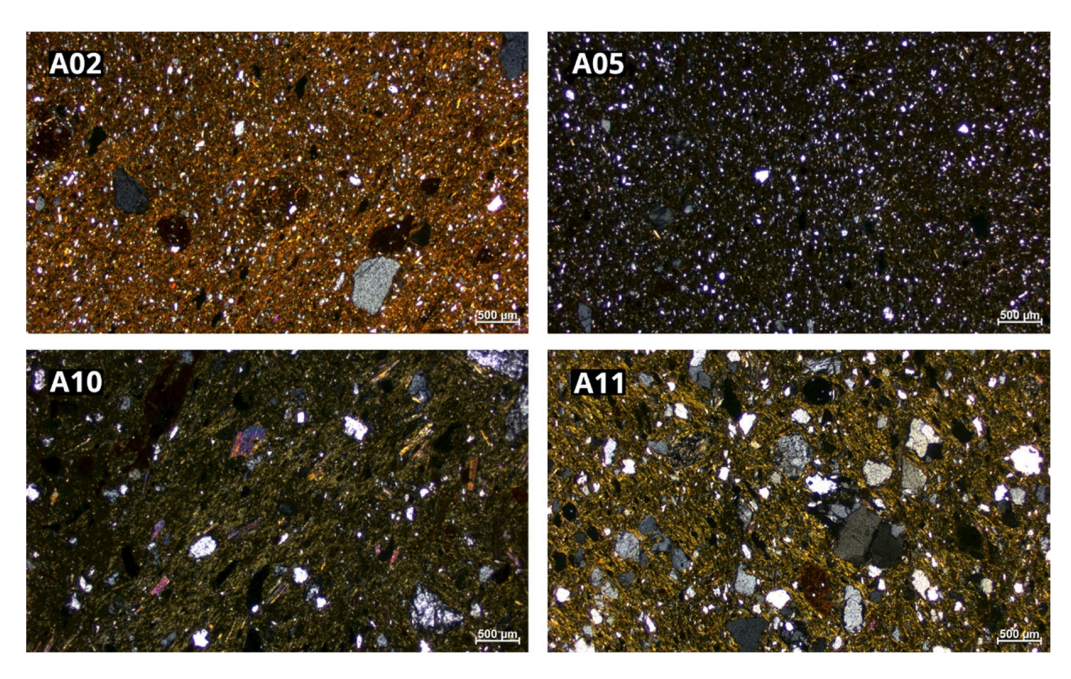


Figure 3. Photomicrographs of ceramic thin sections taken under crossed polars (XPL) at $25 \times$ magnification.

Table 2. Results of the study developed with OM. Mineral and rock fragments identification.

Lab ID	Mineralogy	Rock Fragments	Observations
A01	Qz, K-Fsp, Pl, Ms	Qtzite	Very abundant in Kfs (microcline) and Ms
A02	Qz, K-Fsp, Pl, Ms		Not homogenized Clp identified
A03	Qz, K-Fsp, Pl, Ms		Not homogenized Clp identified
A05	Qz, K-Fsp, Pl, Am, Ms		Rare Am. Not homogenized Clp identified
A06	Qz, K-Fsp, Pl, Ms		
A08	Qz, K-Fsp, Pl, Ms		Not homogenized Clp identified
A09	Qz, K-Fsp, Pl, Ms, Bt (very rare)	Qtzite	Ms-rich
A10	Qz, K-Fsp, Pl, Ms, Bt (very rare)	Qtzite, Clst, Gnrd	Ms-rich
A11	Qz, K-Fsp, Pl, Ms, Bt, Grt	Qtzite, Clst, Gnrd	Ms- and Bt-rich
A12	Qz, K-Fsp, Pl, Ms		Not homogenized Clp identified

Heritage 2025, 8, 405 7 of 14

Table 3. Main characteristics of the ceramic matrix and the porosity.
--

Ceramic Paste				Porosity		
Lab Id Color Hom./Het. Enrichment in Fe or Ca		Optical Activity	Shape and Size			
A01	Brown	Н.НОМ.	Fe	S	Vesicles (meso)	
A02	Red	H.HOM.	Fe	S	Vesicles (meso)	
A03	Red	H.HOM.	Fe	S	Vesicles—Chanels (macro, mega)	
A05	Red	H.HOM.	Fe	S	Vesicles—Chanels (meso, macro)	
A06	Red	Н.НОМ.	Fe	S	Vesicles (micro, macro)	
A08	Red	Н.НОМ.	Fe	S	Vesicles (micro, meso)	
A09	Brown	M.HOM.	Fe	S	Vesicles—Planar voids (meso, macro)	
A10	Brown	M.HOM.	Fe	M	Vesicles—Chanels (meso, macro)	
A11	Brown	M.HOM.	Fe	M	Vesicles—Chanels (meso, macro)	
A12	Red	H.HOM.	Fe	NA	Vesicles (micro, meso)	

H.HOM., highly homogeneous; M.HOM., moderately homogeneous; Fe, iron-rich matrix; S, slightly optically active; M, moderately active; NA, not active.

Table 4. Main characteristics of the temper.

LABID	Temper							
LAB ID Shap	Shape	Sphericity	Packing	Alignment	Sorting	GSD	DGSF	Temper %
A01	G	A-R	CS	Р	M	U	VFS/FS	20
A02	G	A-R	CS	F	W	U	CSilt	10
A03	G	SR-R	CS	F	W	U	CSilt-VFS	20
A05	G	SR-R	CS	F	W	U	CSilt	20
A06	G	SA-R	CS	F	W	U	CSilt	10
A08	G	SR-R	CS	F	W	В	CSilt/CSand	. 10
A09	G/El	A-SR	CS	P	P	В	CSilt/CSand	. 10
A10	G/El	VA-SA	OS	P	P	U	FS	10
A11	G	A-SR	SS	M	M	В	VFS/CSand	10
A12	G	SA-R	CS	F	W	U	CSilt	20

G, mainly granular grains; El, mainly elongated grains. VA, very angular; A, angular; SA, sub-angular; SR, sub-rounded; R, rounded;. CS, close spaced; SS, single spaced; OS, open spaced. P, weak alignment; M, moderate alignment; F, strong alignment. P, poorly sorted; M, moderately sorted; W, well sorted. U, unimodal grain size distribution; B, bimodal. Grain size fractions: VFS, very fine sand; FS, fine sand; CSilt, coarse silt; CSand, coarse sand; VFS/FS, very fine to fine sand; CSilt–VFS, coarse silt to very fine sand; CSilt/CSand, coarse silt and coarse sand; VFS/CSand, very fine and coarse sand.

The first group comprises samples A01, A02, A03, A05, A06, A8, and A12, which exhibit a remarkably homogeneous ceramic matrix characterised by a reddish-brown colour and pronounced optical activity under crossed polarized light. The reddish hue indicates iron oxide enrichment distributed uniformly within the ceramic body. Sample A12 shows an isotropic matrix, consistent with a high degree of vitrification likely linked to elevated firing temperatures/overfiring. Porosity in these samples is mainly represented by vesicles and channels, ranging in size from micro- to macro-scale, reflecting a relatively closed and compact fabric.

The temper consists predominantly of rounded to sub-rounded, equidimensional grains spanning coarse silt to very coarse sand size fractions. Grain size distribution is typically unimodal, with a dominance of finer fractions, although sample A08 displays bimodal distribution. Grain roundness varies from angular to well-rounded, with rounded grains prevailing, indicative of transport and sorting processes prior to incorporation. Temper concentration reaches up to approximately 20%, with inclusions densely and evenly dispersed throughout the matrix. The temper is moderately to well sorted, with grains exhibiting moderate to strong preferred orientation in some samples.

Mineralogically, these samples contain quartz, potassium feldspar, plagioclase feldspar, muscovite, and opaque minerals as primary temper constituents, with occasional amphibole detected (very rare in sample A05). Fragments of quartzite and granitoid lithics were also identified, albeit infrequently. The presence of isolated clay pellets embedded in the matrix suggests incomplete mixing of raw clays or intentional inclusion of specific clay types.

The technological homogeneity across this group implies a shared production tradition, most likely reflecting local ceramic workshops producing different types of amphorae. The consistent presence of small, rounded temper grains—likely intentionally added—and the overall granular fabric suggest that raw clays were subjected to decantation or sieving to remove coarser impurities before forming. The rounded morphology and sorting of inclusions strongly support a fluvial sedimentary origin of the raw materials, consistent with alluvial deposits.

Provenance considerations align with this interpretation, indicating exploitation of clay and temper sources within the Meso-Cenozoic sedimentary basin of the Mondego River, situated near Conímbriga. This basin comprises varied sedimentary lithologies including Quaternary to Cretaceous alluvial sands, sandstones, siltstones, conglomerates, pelites, and subordinate carbonates such as limestones and marls. The chronological distribution of these samples, spanning the 1st to 5th centuries AD, reveals sustained use of these local sedimentary resources throughout the Roman period. Similar results were already obtained by [8].

Conversely, samples A09, A10 and A11 constitute a second group characterised by a coarser, darker brown ceramic matrix, less homogeneous and moderately optically active. Porosity is more pronounced and includes meso- to macro-scale planar voids, vesicles, and channels, indicative of a more open and less compact fabric. Temper content is lower (~10%), composed of a roughly equal mixture of granular and elongated particles with angular to sub-rounded morphologies. Grain size distribution is bimodal, ranging from coarse silt to coarse sand, with a predominance of angular grains and generally weak particle alignment and sorting.

Mineralogical assemblages in this group encompass quartz, potassium feldspar, plagioclase feldspar, muscovite—often exhibiting deformation textures— biotite, garnet in addition to opaque minerals. Lithic inclusions include quartzite, granitoid, and claystone fragments, suggesting a more complex source area. These textural and mineralogical differences indicate a distinct ceramic technology, likely reflecting alternative clay preparation methods and temper selection.

From a geological standpoint, the mineral and lithic inclusions in this second group point towards raw materials derived from the low-grade metamorphic rocks of the Ossa-Morena Zone, located east of the Jurassic sedimentary outcrops. This zone is characterised by Neoproterozoic to Palaeozoic metasedimentary formations such as metagreywackes, meta-conglomerates, meta-cherts, meta-pelites, quartzites, and partially metamorphosed carbonates.

The mineralogical data obtained from powder XRD analysis (Table 5) reveals a broadly consistent firing regime across the assemblage, with quartz emerging as the dominant crystalline phase, accompanied by illite/muscovite, K-rich feldspars, plagioclase feldspars, hematite, biotite, and, in one case, mullite. Sample A11 deviates slightly from this pattern, lacking mullite and instead comprising primarily quartz, illite/muscovite, K-rich feldspars, plagioclase feldspars, and biotite. While garnet was identified petrographically, its absence in the XRD diffractograms is likely attributable to its low abundance and detection limits inherent to the technique.

Lab ID	Qz	Kfs	Pl	Hm	Cal	I/M	Bt	Mul
A01	xxxx	xx		х		xx		
A02	XXXX	X	XX	X	vs	x		
A03	XXXX	vs	vs	X		VS		
A05	XXXX	XX	vs	X		X		
A06	XXXX	XX	vs	X	vs	XX		
A08	XXXX	XX	vs	X		x		
A09	XXXX	XX	vs	vs		x		
A10	XXXX	X	vs	X		XXX		
A11	XXXX	XX	X	X		x	XXX	
A12	XXXX	XX		x				X

Table 5. Mineralogical phases identified by powder XRD.

xxxx = very abundant; xxx = abundant; xx = moderate; x = scarce; vs = traces.

The identification of temperature-sensitive mineral phases provides important insights into the thermal history of the ceramic assemblage [13–15]. The persistence of illite/muscovite, which decomposes at temperatures above 950 $^{\circ}$ C, indicates that most vessels were fired below this threshold. Hematite, typically forming at temperatures above 750 $^{\circ}$ C, was consistently detected, except in sample A12. These observations collectively suggest that the majority of the ceramics were fired within an estimated range of 750–950 $^{\circ}$ C.

Sample A12 is distinctive in its mineralogical profile, exhibiting the absence of illite/muscovite and the presence of mullite—a high-temperature neoformed phase that crystallises at firing temperatures exceeding 1000 °C [16]. This indicates that this vessel was subjected to significantly higher thermal conditions or it was overfired as suggested by OM analysis. Conversely, sample A11, which retains both illite/muscovite and hematite, likely experienced intermediate firing temperatures within the 750–950 °C range. Overall, these data point to a predominantly stable firing tradition with occasional technological variability, possibly reflecting differences in kiln design, fuel management, or functional requirements of specific vessel types.

XRF data provides further support for the differentiation in raw material selection. The two groups identified during optical microscopy analysis show distinctive SiO_2 vs. Al_2O_3 correlation, and Fe_2O_3/Al_2O_3 ratios (Figure 4A,B) indicating that phyllosilicates are important mineralogical phases to consider differentiating ceramics as evidenced by OM and XRD. Trace element data, particularly Zr and Y concentrations (Figure 4C), provide additional diagnostic indicators. Samples A09, A10, and A11 exhibit distinct Zr/Y ratios, implying the use of different tempering materials or clay sources for these vessels.

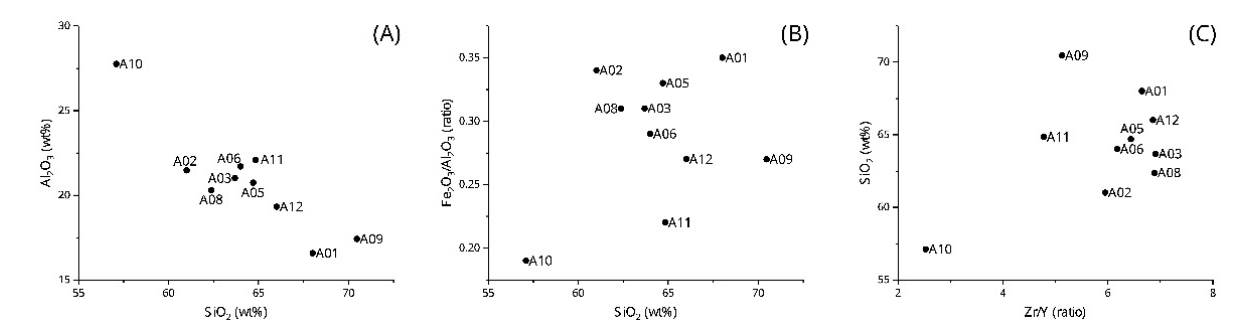


Figure 4. Binary plots of the analysed ceramic samples. (**A**) CaO vs. SiO₂; (**B**) Fe₂O₃/Al₂O₃ vs. SiO₂; (**C**) SiO₂ vs. Zr/Y. These diagrams illustrate compositional variability among the samples and are used to assess raw material sources and potential technological choices.

To further investigate the ceramic microstructure and inclusion characteristics, SEM-EDS analysis was conducted in tandem with the mineralogical and chemical approaches. Most

samples exhibit a dense and homogeneous matrix, with porosity primarily represented by closed vesicles and isolated channels exhibiting low interconnectivity. In contrast, samples A09, A10, and A11 reveal markedly a less compact fabrics, featuring frequent interconnected vugs, channels, and planar voids. These microstructural differences may reflect lower firing temperatures and/or shorter firing durations and are interpreted as indicative of distinct clay processing and firing protocols [17].

Elemental mapping reveals that silicon (Si), aluminium (Al), magnesium (Mg), and iron (Fe) are predominantly concentrated within the ceramic matrix, indicating their incorporation into the fine-grained clay fraction. In contrast, silicon (Si), potassium (K), and sodium (Na) are enriched in the temper grains, particularly within quartz, feldspars, plagio-clases, and muscovite. Calcium (Ca) is generally associated with Na-rich plagioclase, but it is also frequently observed within the pore network, where it likely represents secondary calcite precipitated post-firing due to diagenetic processes. Titanium (Ti) occurs in discrete oxide mineral grains and is occasionally found in association with iron (Fe), suggesting the presence of ilmenite or similar accessory phases.

Of particular note are the large mica crystals—either muscovite or biotite—identified in samples A09, A10, and A11. These inclusions are chemically rich in K, Mg, and Fe and are distributed heterogeneously throughout the ceramic body (Figures 5 and 6). Their frequent occurrence further substantiates the geochemical and microstructural distinctiveness of this subgroup within the broader assemblage, reinforcing interpretations of divergent raw material sources and production techniques.

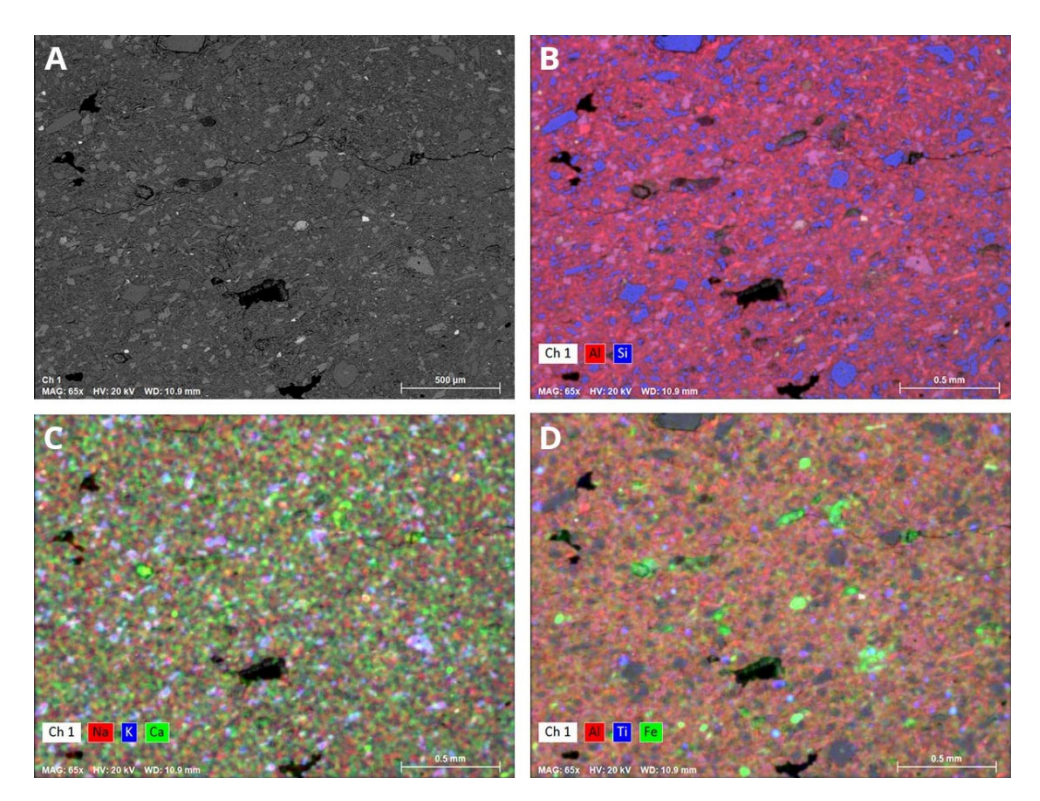


Figure 5. SEM/BSE image and chemical distribution maps of sample A06, showing the microstructural features of the ceramic matrix in backscattered electron (BSE) mode, accompanied by elemental maps highlighting the spatial distribution of key chemical components.

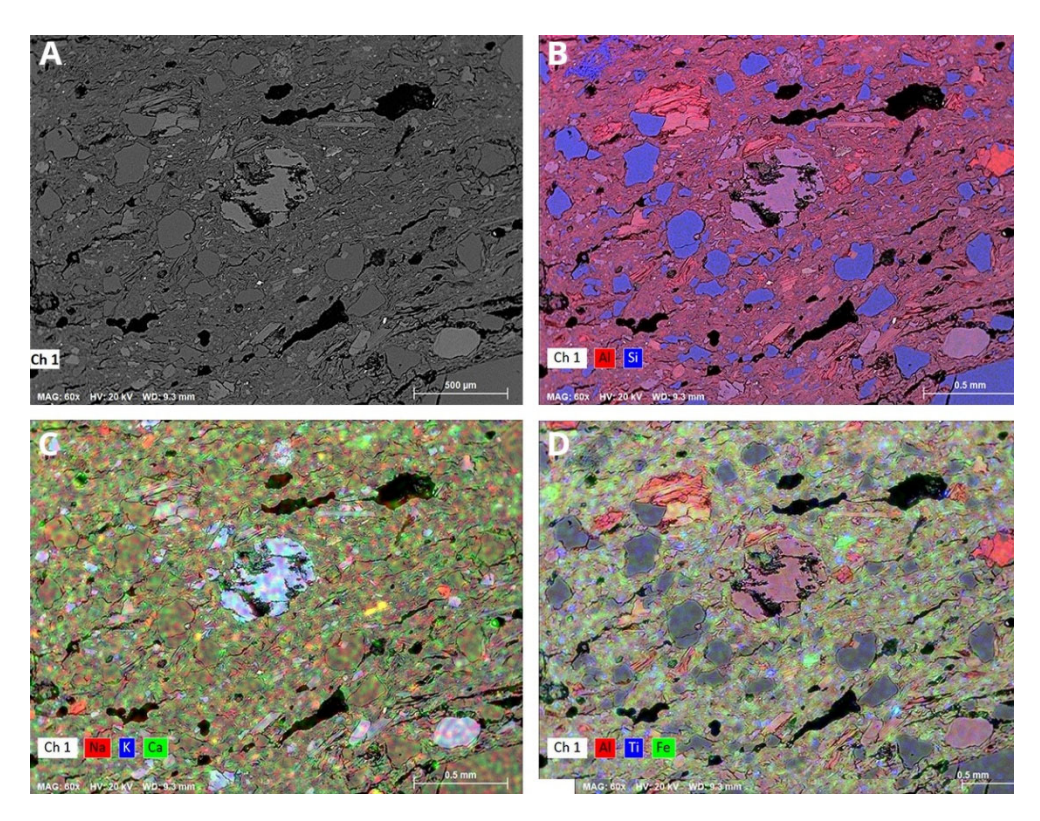


Figure 6. SEM/BSE image and chemical distribution maps of sample A11, showing the microstructural features of the ceramic matrix in backscattered electron (BSE) mode, accompanied by elemental maps highlighting the spatial distribution of key chemical components.

To conclude, the mineralogical, geochemical, and microstructural data reveal significant variability in raw material selection, temper composition, and firing conditions—most notably in samples A09, A10, and A11. However, this variability does not correlate with either the chronological span of the assemblage or the typological classification of the vessels. These findings suggest a broad technological continuity across the period under study. The observed differences are thus more plausibly attributed to functional requirements or workshop-specific production strategies, rather than to temporal or morphological factors.

3.2. Amphora Functionality and Use: Evidence from Organic and Ceramic Data

Four amphorae from the assemblage (A08, A10, A11, and A12) were previously investigated through Gas Chromatography–Mass Spectrometry (GC–MS) and Liquid Chromatography–Tandem Mass Spectrometry (LC–MS/MS), with results disseminated in journals dedicated to regional research [18] and on the evaluation of different and complementary analytical methods for the identification of wine residues [19]. While those studies focused primarily on methodological evaluation, the present paper integrates their outcomes to contextualize the ceramic compositional data and to reassess the functional role of these vessels for an international readership. Given the restricted accessibility of the original publications, a concise summary of the results is provided here.

Sample A12 showed clear evidence of *Pinaceae*-derived pitch, including dehydroabietic and 7-oxo-dehydroabietic acids, simonellite, retene, and related abietane derivatives. Alongside these, abundant lipid markers—1-monopalmitin, 1-monostearin, and undegraded triglycerides such as triolein—indicated the storage of animal fats rather than wine. Sample A08, although lacking resin or wine biomarkers, yielded a degraded lipid spectrum with a predominance of animal fats (P/S ratio = 1.4). The detection of nitrogenous compounds (e.g., hexadecanamide, octadecenamide) points to thermal processing, likely linked to the cooking or preparation of animal products [20,21].

By contrast, A10 and A11 contained levoglucosan, a pyrolysis product of cellulose, together with abietane-type diterpenoids and pimaric acid, suggesting exposure to biomass burning and aged pine resin [22]. These molecular signatures are consistent with heating activities involving plant matter or resin-coated contents.

Taken together, these analyses highlight the multifunctional use of amphorae at Conimbriga: some were coated with resin for liquid storage, while others contained or processed animal fats and plant products. The frequent combination of pitch and lipids underscores their versatile role in transport and storage. At the same time, the absence of certain biomarkers in some samples should be interpreted cautiously, as post-depositional alteration may have obscured original content.

4. Conclusions

This multidisciplinary investigation of the Conímbriga amphorae assemblage provides a nuanced understanding of the technological and functional dimensions of ceramic production and use in Roman Lusitania. By integrating petrographic, mineralogical, geochemical, microstructural, and organic residue data, the study elucidates the interplay among production traditions, raw material sourcing, firing regimes, and vessel functionality.

Two primary technological traditions emerge, distinguished by their distinct raw materials, temper characteristics, and firing conditions. The first tradition is defined by finegrained, well-sorted temper derived from fluvially deposited sediments in the Mondego River basin. These ceramics display high compositional homogeneity and were fired under controlled conditions at moderate temperatures (ca. 750–950 °C), suggesting established workshop protocols and consistent access to local clay resources.

In contrast, the second tradition, exemplified by samples containing coarser, angular inclusions derived from the low-grade metamorphic rocks of the Ossa-Morena Zone, reflects a less refined paste preparation and possibly shorter or lower-temperature firing. This variation suggests the coexistence of alternative production strategies, perhaps associated with distinct workshops, functional requirements, or adaptations to resource availability.

Notably, these technological distinctions do not align with chronological phases or vessel typologies within the assemblage. This lack of correlation implies enduring technological continuity across time and form. Consequently, differences in raw material selection and processing likely reflect functional needs or workshop-specific traditions rather than shifts in ceramic types over time.

The integration of organic residue data reinforces this interpretation. Vessels associated with the fine-grained ceramic tradition—such as A08 and A12—frequently display traces of Pinaceae-derived pitch, indicating deliberate impermeabilization, alongside lipid residues attributable to animal fats, and in at least one case potential wine biomarkers. This combination of features suggests these amphorae were tailored for liquid or semi-liquid contents requiring sealing.

These correlations between technological tradition and vessel use are compelling, though they derive from a limited dataset. Thus, while indicative, they require cautious interpretation. Further research involving larger assemblages and broader contextual data will be essential for verifying and expanding upon these initial patterns.

Overall, this study demonstrates the complexity and diversity of ceramic production and use in Roman Conímbriga, highlighting how technological choices and functional imperatives intersected within local craft and economic systems. By adopting an integrative, multidisciplinary approach, the research advances our understanding of ancient production practices and paves the way for future studies that will further explore the relationships among technology, economy, and material culture in antiquity. Finally, it is important to

underline the importance of optical microscopy analysis (OM), which turned out to be the most informative analysis method employed to evaluate ceramic provenance and technology.

Author Contributions: Data curation: M.B.; Formal analysis I.B., C.O. and M.B.; Funding acquisition I.B., V.H.C. and J.M.; Investigation I.B., C.O., V.H.C. and M.B.; Methodology C.O. and M.B.; Project administration J.M. and M.B.; Resources J.M.; Supervision V.H.C., J.M. and M.B.; Validation C.O., J.M. and M.B.; Writing—original draft I.B., C.O., C.B., V.H.C., N.S. and M.B.; Writing—review and editing I.B., C.O., C.B., V.H.C., N.S., J.M. and M.B. All authors have read and agreed to the published version of the manuscript.

Funding: The archaeometric study was funded by the Center of Cultural and Humanistic Studies of the University of Coimbra (CECH-UC) through the FCT project UIDB/00196/2019.

Data Availability Statement: The data presented in this study is available on request from the corresponding author.

Acknowledgments: Ida Buraca thanks the Foundation for Science and Technology (FCT) for funding her doctoral project "Roman amphorae from the civitas of Conimbriga: supplying a civil center in Lusitânia," carried out in collaboration with the DGPC (FCT/DGPC-PRT/BD/152870/2021). César Oliveira acknowledges the Portuguese Science Foundation (FCT) for his Individual Scientific Employment contract (Doi: 10.54499/2020.00087.CEECIND/CP1593/CT0003). The authors also acknowledge the financial support of HERCULES Laboratory through projects UIDB/04449/2020 (Doi: 10.54499/UIDB/04449/2020) and UIDP/04449/2020 (Doi: 10.54499/UIDP/04449/2020), IN2PAST Associate Laboratory through project LA/P/0132/2020 (Doi: 10.54499/LA/P/0132/2020) and CEAACP—Center for Studies in Archeology, Arts and Heritage (Ref. UIDB/00281/2025), all funded by FCT and by the European Regional Development Fund.

Conflicts of Interest: The authors declare no conflicts of interest.

References

- 1. Correia, V.H. Conimbriga: A Vida de Uma Cidade da Lusitânia; Coimbra University Press: Coimbra, Portugal, 2024.
- 2. Alarcão, J.; Etienne, R. Fouilles de Conimbriga: Alarcão, J.; et al. Céramiques Diverses et Verres; Diffusion de Boccard: Paris, France, 1976; Volume 6.
- 3. Alarcão, P. Construir na Ruína: A Propósito da Cidade Romanizada de Conimbriga; Universidade do Porto: Porto, Portugal, 2009.
- 4. Reis, M.P.; Balneis, D.L.V. Estudo Sobre as Termas e Balneários das Cidades da Lusitânia. Ph.D. Thesis, Universidade de Coimbra, Coimbra, Portugal, 2014. Volume 2.
- 5. Ruivo, J.; Correia, V.H.; Man, A.D. A cronologia da muralha baixo-imperial de Conímbriga. In *Conimbriga Diripitur: Aspetos das Ocupações Tardias de Uma Antiga Cidade Romana*; Ruivo, J., Correia, V.H., Eds.; Coimbra University Press: Coimbra, Portugal, 2021; pp. 15–24.
- 6. Ruivo, J.; Correia, V.H. *Conimbriga Diripitur: Aspetos das Ocupações Tardias de Uma Antiga Cidade Romana*; Coimbra University Press: Coimbra, Portugal, 2021; Volume 67.
- 7. De Man, A.; Soares, A.M. A datação pelo radiocarbono de contextos pós-romanos de Conimbriga. *Rev. Port. Arqueol.* **2007**, *10*, 285–294.
- 8. Alarcão, J. Fouilles de Conimbriga V, in La Céramique Commune Locale et Régionale; Diffusion de Boccard: Paris, France, 1975.
- 9. Correia, V.H.; Man, A.D. Variação e Constância na Ocupação de Conimbriga e do seu Território; CIDEHUS: Évora, Portugal, 2010.
- 10. Correia, V.H.; Buraca, I.; Triães, R.; Oliveira, C. Identificação de uma produção de ânforas romanas no norte da Lusitânia. *Rev. Port. Arqueol.* **2015**, *18*, 136–225.
- 11. Quinn, P.S. Ceramic Petrography: The Interpretation of Archaeological Pottery & Related Artefacts in Thin Section; Archaeopress Publishing Ltd.: Oxford, UK, 2013.
- 12. Wentworth, C.K. A Scale of Grade and Class Terms for Clastic Sediments. J. Geol. 1922, 30, 377–392. [CrossRef]
- 13. Riccardi, M.; Messiga, B.; Duminuco, P. An approach to the dynamics of clay firing. Appl. Clay Sci. 1999, 15, 393–409. [CrossRef]
- 14. Gliozzo, E. Ceramic technology. How to reconstruct the firing process. Archaeol. Anthropol. Sci. 2020, 12, 260. [CrossRef]
- 15. Maritan, L.; Nodari, L.; Milano, A.; Russo, U. Influence of firing conditions on ceramic products: Experimental study on clay rich in organic matter. *Appl. Clay Sci.* **2006**, *31*, 1–15. [CrossRef]

16. Heimann, R.B.; Maggetti, M. The struggle between thermodynamics and kinetics: Phase evolution of ancient and historical ceramics. In *The Contribution of Mineralogy to Cultural Heritage*; Artioli, G., Oberti, R., Eds.; European Mineral Union and the Mineralogical Society of Great Britain & Ireland: Twickenham, UK, 2019; pp. 233–281.

- 17. Xanthopoulou, V.; Iliopoulos, I.; Liritzis, I. Mineralogical and Microstructure Analysis for Characterization and Provenance of Ceramic Artifacts from Late Helladic Kastrouli Settlement, Delphi (Central Greece). *Geosciences* **2021**, *11*, 36. [CrossRef]
- 18. Oliveira, C.; Buraca, I.; Correia, V.H.; Triães, R. Análises químicas de ânforas identificadas em Conímbriga. *Al-Madan* **2015**, 19, 175–176.
- 19. Buraca, S.I.; Olveira, C.J.S.; Elesi, G.; Connan, J.; Morais, R.; Correia, V.H. In Vino veritas. An assessment of current research of amphorae contents from Conimbriga (Portugal). *DIAITA Food* **2025**, 2, e0207. [CrossRef] [PubMed]
- 20. Lejay, M.; Alexis, M.A.; Quenea, K.; Anquetil, C.; Bon, F. The organic signature of an experimental meat-cooking fireplace: The identification of nitrogen compounds and their archaeological potential. *Org. Geochem.* **2019**, *138*, 103923. [CrossRef]
- 21. Lejay, M.; Alexis, M.; Quénéa, K.; Sellami, F.; Bon, F. Organic signatures of fireplaces: Experimental references for archaeological interpretations. *Org. Geochem.* **2016**, *99*, *67–77*. [CrossRef]
- 22. Correia, V.H.; Buraca, I.; Triães, R.; Araújo, A.; Oliveira, C. Identification of a production of Roman amphorae in Northern Lusitania. In *Archaeo Analytics—Chromatography and DNA Analysis in Archaeology*; Oliveira, C., Morais, R., Cerdán, Á.M., Eds.; Esposende City Council: Esposende, Portugal, 2015; pp. 169–184.

Disclaimer/Publisher's Note: The statements, opinions and data contained in all publications are solely those of the individual author(s) and contributor(s) and not of MDPI and/or the editor(s). MDPI and/or the editor(s) disclaim responsibility for any injury to people or property resulting from any ideas, methods, instructions or products referred to in the content.